Tailoring Conducting Polymer Chemistry for the Chemical Deposition of Metal Particles and Clusters

Hsing-Lin Wang,*,† Wenguang Li,† Q. X. Jia,‡ and Elshan Akhadov‡

C-PCS, Chemistry Division and Materials Physics and Application Division, Los Alamos National Laboratory, Los Alamos, New Mexico 87545

Received August 18, 2006. Revised Manuscript Received November 28, 2006

We report chemical deposition of metal particles and clusters with various sizes and morphologies on top of the polyaniline (PANI) thin films and porous asymmetry membranes. Immersing the PANI membrane into the $PtCl_4^{2-}$ gives rise to 3−5 nm Pt nanoparticles spread evenly on the membrane surface, while immersing undoped PANI membrane into $AgNO_3$ aqueous solution leads to the formation of micrometer size Ag sheets with strong anisotropy. In contrast to the Ag deposited on the undoped PANI membrane, Ag metal deposited on the doped PANI membrane has a random morphology and shows no preferential growth along a specific crystallographic direction. The Au metal deposited on the undoped and doped PANI membranes exhibit morphological differences from a sheetlike structure to larger particles comprised of smaller Au particulates (rice-grain shape). Furthermore, by varying the nature of the dopant, we can achieve deposition of metal structures with fiber, sheet, cube, yarn-ball, and leaf-like morphologies. Our studies demonstrate that tunable metal size and morphology can be easily achieved through tailoring the surface chemistry of conducting polymer by varying the dopant, oxidation state (doped and undoped), and polymer chain orientation. Our future goal is to further enhance the control over metal structure and morphology using a simple chemical deposition method.

Introduction

In the past few decades, there has been an increasing interest in using conducting polymers to fabricate electronic and optical devices such as light-emitting diodes[1,2] and molecular electronics.[3,4] Polyaniline (PANI), being one of the most commonly used conducting polymers due to its facile synthesis, lower price tag, and environmental stability, has been extensively studied for its use as electromagnetic shielding[5−7] and anticorrosion coating.[8−11] The redox potential accompanying the color change makes it an ideal candidate for making electrochromic devices. An earlier study by Gustafsson et al. demonstrates that highly conductive PANI thin films can be used as transparent electrodes for fabrication of flexible light-emitting diodes (LEDs). Furthermore, they showed that the high surface contact with the polymeric emitter also results in lower turn-on voltage and higher quantum efficiency.[12] Many of these devices involve understanding and controlling the electron transfer at the interface between conjugated polymer and metal electrodes. Therefore, better understanding the interfacial phenomena between conducting polymers and metals remains an area of interest for fabricating efficient devices. Besides the application in fabricating electronic and optical devices, PANI films have shown potential in chemical separations. For example, Anderson et al. used PANI thin films to generate concentrated gases via a molecular sieving mechanism.[13,14] The efficacy of generating concentrated gases using PANI films is mainly determined by the size of the chemicals and their affinity toward PANI. To enhance the separation efficiency, we have fabricated PANI porous asymmetry membranes with a very thin dense skin ($<1\ \mu$m) and a porous sublayer, allowing the gases to permeate in a minimum time period. These membranes are prepared using a phase inversion process[15,16] where a wet PANI film is immersed into a coagulation bath containing nonsolvents

* Corresponding author. E-mail: hwang@lanl.gov.
† Chemistry Division.
‡ Materials Physics and Application Division.

(1) Burroughes, J. H.; Bradley, D. D. C.; Brown, A. R.; Marks, R. N.; Mackay, K.; Friend, R. H.; Burns, P. L.; Holmes, A. B. *Nature* **1990**, *347* (6293), 539−41.
(2) Burn, P. L.; Holmes, A. B.; Kraft, A.; Bradley, D. D. C.; Brown, A. R.; Friend, R. H.; Gymer, R. W. *Nature* **1992**, *356* (6364), 47−9.
(3) Campbell, I. H.; Kress, J. D.; Martin, R. L.; Smith, D. L.; Barashkov, N. N.; Ferraris, J. P. *Appl. Phys. Lett.* **1997**, *71* (24), 3528−30.
(4) Chen, S. A.; Fang, Y. *Angew. Makromol. Chem.* **1993**, *208*, 79−86.
(5) Maekelae, T.; Pienimaa, S.; Taka, T.; Jussila, S.; Isotalo, H. *Synth. Met.* **1997**, *85* (1−3), 1335−6.
(6) Epstein, A. J. *MRS Bull.* **1997**, *22* (6), 16−22.
(7) Koul, S.; Chandra, R.; Dhawan, S. K. *Polymer* **2000**, *41* (26), 9305−10.
(8) Li, P.; Tan, T. C.; Lee, J. Y. *Synth. Met.* **1997**, *88* (3), 237−42.
(9) Wessling, B. *Adv. Mater.* **1994**, *6* (3), 226−8.
(10) Trochnagels, G.; Winand, R.; Weymeersch, A.; Renard, L. *J. Appl. Electrochem.* **1992**, *22* (8), 756−64.
(11) Sathiyanarayanan, S.; Dhawan, S. K.; Trivedi, D. C.; Balakrishnan, K. *Corros. Sci.* **1992**, *33* (12), 1831−41.
(12) Gustafsson, G.; Cao, Y.; Treacy, G. M.; Klavetter, F.; Colaneri, N.; Heeger, A. J. *Nature* **1992**, *357* (6378), 477−9.
(13) Anderson, M. R.; Mattes, B. R.; Reiss, H.; Kaner, R. B. *Science* **1991**, *252* (5011), 1412−5.
(14) Anderson, M. R.; Mattes, B. R.; Reiss, H.; Kaner, R. B. Gas separation membranes - a novel application for conducting polymers. In *Proceedings of the International Conference on Science and Technology of Synthetic Metals (ICSM '90), Tubingen, F.R.G., September 2−7, 1990*; Elsevier: Lausanne, Switzerland, 1991; Vol. 41 (3), pp 1151−4.
(15) Loeb, S.; Sourirajan, S. *Adv. Chem. Ser.* **1962**, *38*, 117.
(16) Kesting, R. E.; Menefee, A. *Kolloid Z. Z. Polym.* **1969**, *230* (2), 341−6.

10.1021/cm0619508 CCC: $37.00
Published on Web 01/11/2007

(e.g., water and methanol).[17] In this paper, we show that these porous membranes are a great material for chemical deposition of metal particles and clusters on their surfaces.

PANI possesses secondary amines and tertiary imines in the backbone structure that can bind metal ions; these metal ions can be released by immersing ion-bound PANI into a low pH solution. The ability of binding metal ions and subsequent liberation makes PANI an attractive material for environmental remediation. In the cases where metal ions have a reduction potential higher than that of the PANI, the bound metal ions can be reduced to form zerovalent metals. Therefore, it was long recognized that PANI can be used for electrodeless precipitation of metals from a metal ion solution.[18] Kang and colleagues showed reduction and precipitation of gold from acid solution using conducting polymers.[19] Huang et al. demonstrated metallization of printed-circuit boards using polyaniline.[20] Although the electrodeless deposition of metals using conducting polymer have been demonstrated, *understanding and controlling the growth of metal structure on conducting polymer surfaces are still lacking*. In our laboratory, we recently demonstrated synthesis of metal nanoparticles using conducting polymer colloids.[21,22] These as-synthesized metal nanoparticles can either spread throughout the solution or be embedded in the conducting polymer colloids to form a novel composite material.[22] In the process of reducing metal ions to form metal nanoparticles, the oxidation state of PANI changes from emeraldine base form to a more oxidized pernigraniline base form.[22] Therefore, PANI serves the role of an electron donor. Here, we show chemical deposition and characterization of metals and metal particles and clusters on the PANI surfaces. Our results show various metal structures, sizes, and morphologies as we alter PANI's redox states and dopants. In addition, we show that preferential deposition of Ag coincides with the direction of stretched aligned PANI presumably due to lower reduction potential. Preferential deposition of metals on a conductive substrate provides a new way to pattern metal structures for device fabrication.

Materials

Polyaniline emeraldine base (EB) powder was obtained from Neste Oy. *N*-Methyl-2-pyrrolidone (99% Aldrich), heptamethylenimine (98% Acros), $AgNO_3$ (99+% Aldrich), $AuCl_3$ (99.9% Aldrich), and K_2PtCl_4 (99.9% Aldrich) were used without further purification.

Fabrication of Porous Asymmetric Membranes and Dense Films. Fabrication of PANI porous asymmetric membranes is achieved by employing the phase inversion method using water as the coagulation bath. In a typical procedure, 3.70 g of NMP (99% Aldrich, dried by a 4 Å molecular sieve) was placed into a 12.0 mL Teflon vial. Then 0.31 g of heptamethylenimine (HPMI, 98% Acros) was added to it. The vial was sealed with a Teflon cap and kept in an oven at 60 °C for 5 min. Then 1.00 g of EB powder was added to the vial. The solution was slowly stirred with a homogenizer and then ramped up to 5000 rpm for 25 min. The EB/HPMI molar ratio was 1:1 (the moles of EB are calculated based on the tetrameric repeat unit). The resulting EB solution was poured onto a glass plate and spread onto a wet film using a gardener's blade (Pompano Beach, FL) with a preset thickness. The porous membranes were prepared by immersing and holding the wet films in the water bath for more than 24 h. The resulting membrane was then dried under vacuum at room temperature for 12 h before any subsequent processing. The PANI dense films were prepared by placing the wet films into a 60 °C oven overnight to allow solvent evaporation and the thermally cured dense films were then placed into a water bath for 24 h to remove the residue solvent. These PANI substrates were then immersed in a 0.1 M aqueous acid solution for ~24 h followed by immersion into metal-ion solutions for time periods ranging from several minutes to 24 h depending on the rate of reaction. One hundred millimolar metal-ion solutions were prepared using as-purchased $AgNO_3$, $AuCl_3$, and K_2PtCl_4 without further purification.

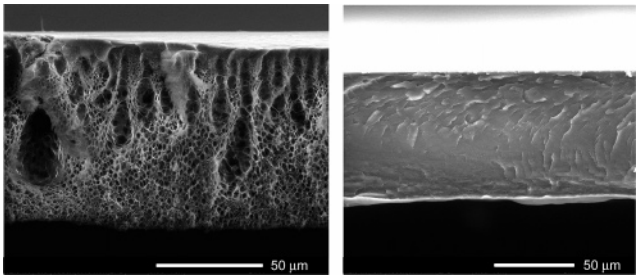

Figure 1. SEM micrographs of a cross section of a porous asymmetric membrane (left) and a thermally cured dense film (right).

The structure of the doped PANI membranes and deposited metals were studied by X-ray diffraction (XRD) with a Siemens D5000 four-circle diffractometer with Cu Kα radiation (λ = 0.15418 nm). Normal $\theta-2\theta$ scans were performed on these samples to determine their crystallographic orientation. SEM micrographs of metals on the PANI membrane surfaces were taken using a JEOL 6300FXV SEM and FEI Quanta 400 FEG ESEM.

Results and Discussion

Using PANI porous membranes for chemical deposition has the advantage of lower density as compared to that of the thermally cured dense films. The structure and mechanical properties of PANI membranes have been well-characterized using a wide range of spectroscopic and microscopic techniques and were used to fabricate high-performance, monolithic actuators.[17,23,24] Figure 1 shows clear contrast between the PANI dense film and porous membrane. The lower density allows diffusion of metal ions between PANI chains and hence facilitation of the nucleation process. More importantly, the PANI membranes prepared by the phase inversion process does not involve heat treatment for a prolonged time period. The phase inversion process allows PANI to maintain its original redox states and prevents the

(17) Wang, H. L.; Gao, J. B.; Sansinena, J. M.; McCarthy, P. *Chem. Mater.* **2002**, *14* (6), 2546−52.
(18) Ting, Y. P.; Neoh, K. G.; Kang, E. T.; Tan, K. L. *J. Chem. Technol. Biotechnol.* **1994**, *59*, 31−6.
(19) Kang, E. T.; Ting, Y. P.; Tan, K. L. *J. Appl. Polym. Sci.* **1994**, *12* (53), 1539−45.
(20) Huang, W. S.; Angelopoulos, M.; White, J. R.; Park, J. M. *Mol. Cryst. Liq. Cryst.* **1990**, *189*, 227−35.
(21) Li, W. G.; McCarthy, P. A.; Liu, D. G.; Huang, J. Y.; Yang, S. C.; Wang, H. L. *Macromolecules* **2002**, *35* (27), 9975−82.
(22) Li, W.; Jia, Q. X.; Wang, H.-L. *Polymer* **2006**, *47* (1), 23−6.
(23) Gao, J. B.; Sansinena, J. M.; Wang, H. L. *Chem. Mater.* **2003**, *15* (12), 2411−8.
(24) Wang, H. L.; Romero, R. J.; Mattes, B. R.; Zhu, Y. T.; Winokur, M. J. *J. Polym. Sci., Part B: Polym. Phys.* **2000**, *38* (1), 194−204.

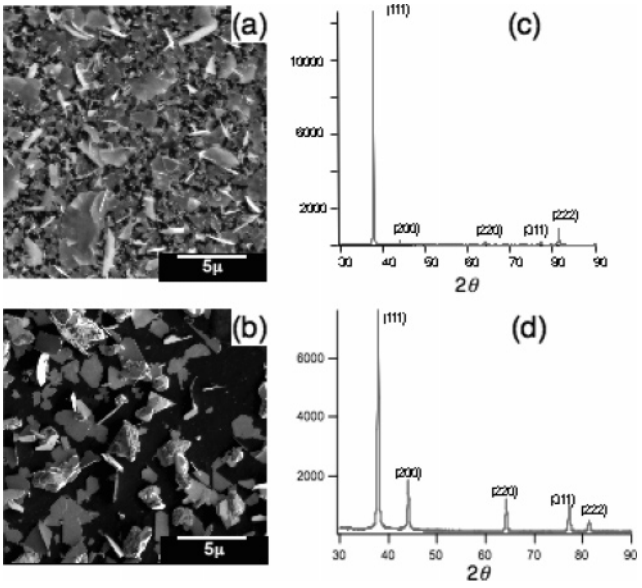

Figure 2. SEM micrographs and X-ray diffraction of Ag on the undoped PANI (top) and HCl-doped (bottom) PANI surfaces.

potential cross-linking between PANI chains.[25,26] We believe this is one of the reasons that we observe the differences in metal morphologies grown from the thermally cured dense films and the porous membranes. Deposition of metals on top of PANI surfaces is simply achieved by immersing the prefabricated PANI membranes or thermally cured dense films into a metal ion aqueous solution with ion concentrations ranging from 0.01 to 1.0 M. The time period for the metal growth ranges from several seconds to several hours depending on the experimental conditions such as temperature and metal ion concentration. The membranes are left in the solution until the metal deposition is visually observed on the membrane surfaces.

Figures 2a and b show the SEM images of the evenly distributed Ag metal grown on top of the undoped and doped PANI membranes and the morphological differences between the two are obvious. Figure 2a shows very thin Ag sheets spread evenly on top of the PANI membrane surface. Higher surface coverage of Ag sheets on the undoped PANI membrane suggests favorable interaction between Ag and the undoped PANI. Furthermore, most of the silver sheets have an estimated thickness of less than a few nanometers, appearing as transparent during high-voltage SEM imaging. In contrast to the Ag sheets on the undoped PANI membrane, Ag on the HCl-doped membrane has a random morphology. Silver sheets with thickness of ~20 nm and large globular Ag particulates occupy the membrane surface with approximately equal distribution. The SEM image also reveals less surface coverage of Ag on the doped PANI membrane. The presence of silver is further confirmed by the XRD spectra, clearly identifying the five silver peaks, as shown in Figures 2c and 2d. In addition to the difference in morphology, XRD spectra also indicate anisotropy of Ag on the undoped membrane surface (Figure 2c). XRD scan

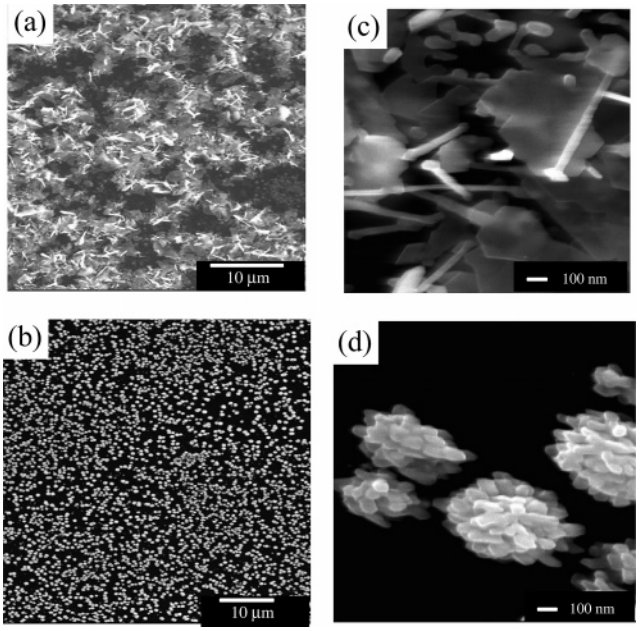

Figure 3. SEM micrographs of Au deposition on the undoped (a) and the doped (b) PANI membranes surfaces. (c) and (d) are the magnified SEM micrographs of (a) and (b), respectively.

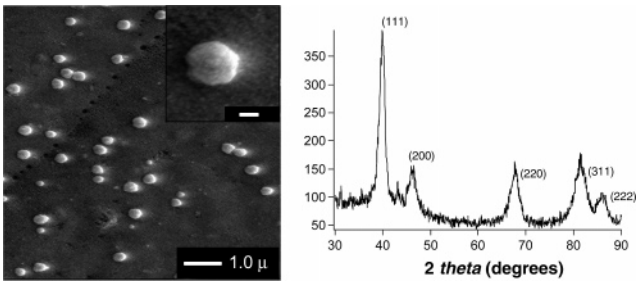

Figure 4. SEM micrograph (left) and the X-ray diffraction (right) of Pt nanoparticles deposited on the undoped PANI membrane. Inset shows that the larger Pt cluster consists of an ensemble of smaller nanoparticles (scale bar 100 nm).

of these Ag sheets on the undoped PANI surface clearly shows (111) and (222) preferential orientation since (200), (220), and (311) peaks are barely above the background signal. The above results suggest that Ag sheets on the undoped PANI surface preferentially grow along the [111] direction. We show in this study deposition of Ag metal with different structures and morphologies can be achieved by simply varying the doping state of the PANI membrane.

Following the same procedures, we perform chemical deposition of Au metal on the PANI membrane surface (see Figure 3). In this study, we observe mostly Au sheets along with some scattered nanoparticles (~100 nm) on the undoped PANI membrane. High surface coverage indicates favorable interaction between Au sheets and undoped PANI, resembling the Ag deposition on the undoped PANI. Deposition of Au on the doped PANI membrane exhibits a uniform morphology with evenly dispersed Au particulates on the membrane surface. The magnified SEM image (Figure 3d) reveals submicrometer-size Au particulates that are in fact conglomerates of smaller Au nanoparticles with a rice-grain morphology. The size of these conglomerates is determined by the total number of smaller rice-grain Au particles.

Pt ions can also be reduced by PANI to form Pt metal due to its higher reduction potential compared to that of the

(25) Wei, Y.; Hsueh, K. F. *J. Polym. Sci., Part A: Polym. Chem.* **1989**, *27* (13), 4351−63.
(26) Milton, A. J.; Monkman, A. P. *J. Phys. D (Appl. Phys.)* **1993**, *26* (9), 1468−74.

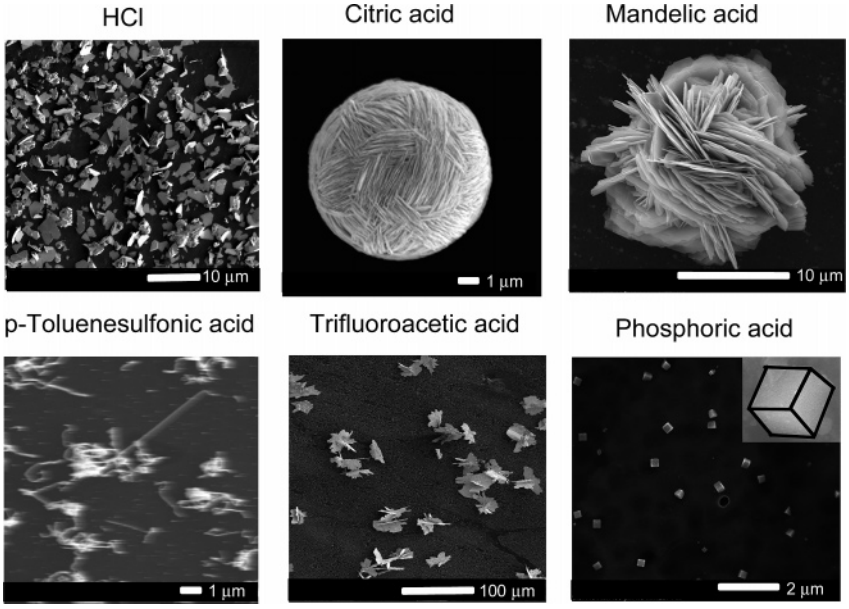

Figure 5. SEM micrographs of Ag on PANI surfaces doped with various acids. Inset shows the magnified Ag cubes on a phosphoric acid-doped PANI surface.

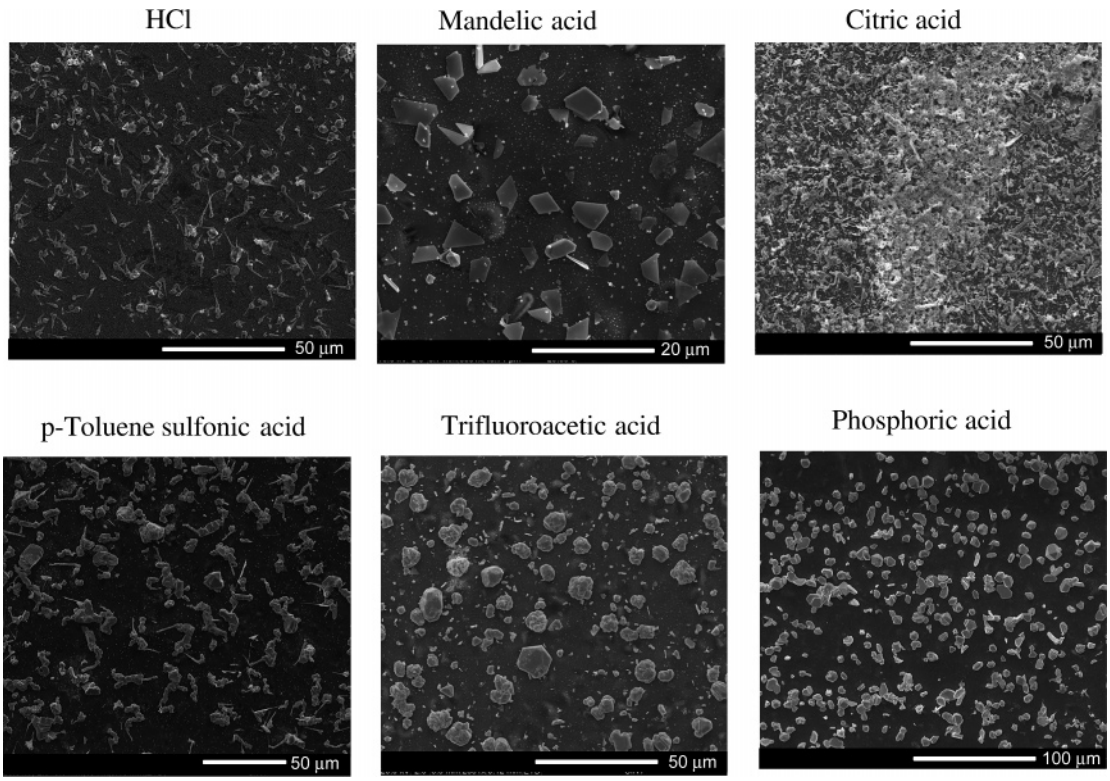

Figure 6. SEM micrographs of Ag on the surfaces of thermally cured PANI dense films doped with various acids.

PANI.[22] Deposited Pt metal on the undoped PANI membrane surface appears as a layer of Pt nanoparticles along with some large Pt clusters with an estimated size distribution from ~100 to 300 nm (see Figure 4). Close examination of these large clusters (inset of Figure 4) indicates that they are conglomerates of an ensemble of much smaller Pt nanoparticles. Although we cannot clearly determine the exact dimension and size distribution of these nanoparticles, high-resolution SEM indicates that most of these nanoparticles are less than 10 nm. This result is further confirmed by the XRD spectrum of a Pt-coated PANI membrane, which not only shows diffraction peaks from different crystallographic orientations but also reveals a very broad full-width at half-maximum from each diffraction peak. The particle size calculated based on the extra breadth or broadening due to the particle-size effect alone from X-ray diffraction lines is ~5 nm, which agrees well with the high-resolution SEM results. One may argue that the XRD peaks of these larger Pt clusters may have been overwhelmed by the much smaller nanoparticles. Our previous study indicates that larger particles often dominate the overall XRD spectrum as they show a much sharper peak with high intensity.[22] These broad XRD peaks suggest that the larger Pt cluster is indeed made up of many Pt nanoparticles. The above result also implies,

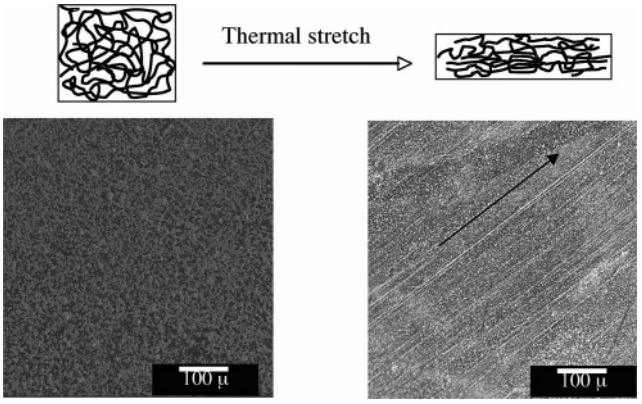

Figure 7. SEM micrograph of homogeneously dispersed Ag particles deposited on the unstretched PANI film (left) compared to that of Ag deposition preferentially along the stretched direction (right). Arrow shows stretched direction.

for the first time, Pt nanoparticles can be made simply by immersing PANI porous membrane into a $PtCl_4^{2-}$ aqueous solution. We speculate that the very small difference in reduction potential (~0.05 V) between PANI and $PtCl_4^{2-}$ may have resulted in slower nucleation rate, which then leads to the formation of smaller nanoparticles.

In an attempt to better understand how the nature of dopants impacts the final structure and morphology of metal on the PANI membranes, we doped six pieces of PANI membranes (cut from one larger piece) with HCl, H_3PO_4, CF_3COOH, citric acid, mandelic acid, and *p*-$CH_3C_6H_5SO_3H$. These membranes were then immersed into 0.01 M $AgNO_3$ solution. The resulting Ag metal exhibits completely different morphologies, as illustrated in Figure 5. Ag grown on a HCl-doped PANI membrane surface has a random morphology, while Ag deposited on citric acid-doped PANI membrane exhibits a yarn-ball morphology. Note that, upon close examination, it is apparent that this hemispheric yarn ball is not comprised of Ag nanowires, but rather it consists of close-packed silver sheets with a thickness of ~25 nm, similar to that of the Ag grown on a mandelic acid-doped membrane surface. Ag nanowires of 20 nm in diameter are observed on the *p*-toluenesulfonic acid-doped membrane surface. Ag grown on the trifluoroacetic acid-doped membrane has a leaf-like morphology. Finally, the Ag deposited on the phosphoric acid-doped membrane looks like sugar cubes with characteristic dimension of 200 nm. All the above Ag metals were carefully characterized and identified using X-ray diffraction and energy dispersive X-ray analysis (results not shown here). The five peaks in X-ray diffraction spectra assigned as (111), (200), (220), (311), and (222) are positively identified to ensure the metal particles deposited on the PANI membrane surface are indeed Ag rather than Ag salt. The above results demonstrate the potential of controlling the size and morphology of metal particles by varying the nature of the dopant.

Metal deposition on the membrane surfaces through reduction requires electron transfer from PANI to metal ions. As the metal ions approach the PANI surfaces, they are reduced by PANI and form nuclei. In a homogeneous system, where metal ions and reducing agent are dispersed in solution, the metal nuclei serve as catalytic sites for surface growth, allowing the formation of larger metal structures.[27] In a heterogeneous system, where metal ions are reduced on a membrane surface, the growth mechanism may differ from the homogeneous systems. The size of metal nuclei is likely to be dominated by the difference in reduction potential between metal ions and the PANI[22] and by the surface properties of the substrates. The morphological difference corresponding to various dopants may be influenced by the surface energy of the membrane (manifested by the water contact angles) which can be tuned by the nature of the dopants and the redox states of the PANI membrane.[17]

Morphological differences could also be due to the difference in composition and structure (lattice space) resulting from incorporating dopants into the PANI membrane. For example, the incorporated dopants change the interchain spacing, which could favor the growth of metal along a specific direction if the lattice parameters match the interchain distance. Unfortunately, the XRD spectra of the above doped membranes and Ag deposited on the membrane surfaces do not provide conclusive evidence in revealing the hypothesized mechanism. As of now, how the growth mechanism relates to the dopant-dependent morphology remains unknown. Our results reveal a minor effect of metal ion concentration on the final structure and morphology of metals deposited on the PANI surfaces. Prolonged exposure of PANI membrane to the metal ion solution does not change the morphology; it only slightly increases the density of metal deposited on the membrane surface. The above results suggest that the metal deposition on the membrane surface is dominated by a thermodynamic process, i.e., the energy required to reduce the metal ions to form metal.

For the sake of comparison, we have grown metals on the thermally cured dense films. The metals grown on the thermally cured dense film exhibits less variation in their morphologies (see Figure 6). In general, the Ag growth on top of the PANI dense films doped with six different acids exhibits large structures, greater than a few microns, with random morphology. The only exception is the mandelic acid-doped PANI film which grows large Ag platelets with a thickness of ~20 μm. Another interesting observation is that all of the acid-doped PANI films exhibit growth of nanocubes with the dimensions ranging from 60 to 200 nm, similar to that of the Ag nanocubes grown on top of the phosphoric acid-doped PANI membrane. Most of these nanocubes are very small and a large number of them on the PANI surfaces make these films appear cloudy.

Another level of control over the metal growth can be realized by using the stretched PANI films (4 times its original length). The contrast between Ag deposited on the stretched and unstretched PANI films is clearly shown in Figure 7. We observe a preferential deposition of Ag on the PANI surface coinciding with the stretched direction. In contrast, the unstretched film exhibits homogeneous Ag deposition throughout the PANI surface. This preferential Ag deposition is likely due to lower reduction potential of the stretched oriented PANI. The stretched (extended) PANI chain conformation leads to the formation of crystalline

(27) Watzky, M.; Finke, R. *Chem. Mater.* **1997**, *9* (12), 3083−95.

regions with lower reduction potential and higher conductivity than that of the unstretched parts.[28−31]

Conclusion

We have demonstrated ways for controlling the formation of metals on reductive PANI surfaces by tailoring their surface chemistry and redox potentials. A wide range of Ag morphologies induced by different dopants, ranging from fiber, sheet, cube, to hemispheric yarn ball, have been observed. The sizes of these deposited metal structures range from a few nanometers to several micrometers while the metal ion concentration and the exposure time do not impact the metal morphology, suggesting that the metal growth is largely governed by a thermodynamic mechanism. This hypothesis is consistent with observed results that reveal a small difference in reduction potential between Pt^{2+} and PANI, leading to the growth of monodispersed 5 nm Pt nanoparticles spread evenly on top of the PANI surface. In addition, we demonstrate a method for preferential deposition of Ag on the stretched aligned PANI thin film. Facile synthesis of metal particles and clusters on reductive substrate surfaces have great potential in highly efficient catalytic surfaces and in low-cost devices associated with high sensitivity detection using SERS.

Acknowledgment. The authors are thankful for the financial support from the Cross Enterprise Technology Development Program of the National Aeronautics and Space Administration (NASA) and the Office of Science (DOE). Partial support from the Laboratory Directed Research and Development (LDRD) fund is also greatly appreciated. This work was performed in part at the U.S. Department of Energy, Center for Integrated Nanotechnologies, at Los Alamos National Laboratory (Contract DE-AC52-06NA25396) and Sandia National Laboratories (Contract DE-AC04-94AL85000).

CM0619508

(28) Abell, L.; Adams, P. N.; Monkman, A. P. *Polymer* **1996**, *37* (26), 5927−31.
(29) Jeong, S. K.; Suh, J. S.; Oh, E. J.; Park, Y. W.; Kim, C. Y.; MacDiarmid, A. G. *Synth. Met.* **1995**, *69* (1/3), 171−2.
(30) Adams, P. N.; Devasagayam, P.; Pomfret, S. J.; Abell, L.; Monkman, A. P. *J. Phys.: Condens. Matter* **1998**, *10* (37), 8293−303.
(31) McCall, R. P.; Scherr, E. M.; MacDiarmid, A. G.; Epstein, A. J. *Phys. Rev. B (Condens. Matter)* **1994**, *50* (8), 5094−100.